frontiers in
PSYCHIATRY

METHODS ARTICLE
published: 10 October 2011
doi: 10.3389/fpsyt.2011.00054

Use of high resolution 3D diffusion tensor imaging to study brain white matter development in live neonatal rats

Yu Cai[1,2], Matthew S. McMurray[3], Ipek Oguz[3,4], Hong Yuan[1,2], Martin A. Styner[3,4], Weili Lin[1,2], Josephine M. Johns[3,4] and Hongyu An[1,2]*

[1] *Department of Radiology, University of North Carolina at Chapel Hill, Chapel Hill, NC, USA*
[2] *Biomedical Research Imaging Center, University of North Carolina at Chapel Hill, Chapel Hill, NC, USA*
[3] *Department of Psychology, University of North Carolina at Chapel Hill, Chapel Hill, NC, USA*
[4] *Department of Psychiatry, University of North Carolina at Chapel Hill, Chapel Hill, NC, USA*

Edited by:
Sheryl Moy, University of North Carolina, USA

Reviewed by:
Istvan Pirko, Mayo Clinic, USA

****Correspondence:***
Hongyu An, Department of Radiology, University of North Carolina at Chapel Hill, 106 Mason Farm Road, CB#7515, Chapel Hill, NC 27599, USA.
e-mail: hongyuan@med.unc.edu

High resolution diffusion tensor imaging (DTI) can provide important information on brain development, yet it is challenging in live neonatal rats due to the small size of neonatal brain and motion-sensitive nature of DTI. Imaging in live neonatal rats has clear advantages over fixed brain scans, as longitudinal and functional studies would be feasible to understand neuro-developmental abnormalities. In this study, we developed imaging strategies that can be used to obtain high resolution 3D DTI images in live neonatal rats at postnatal day 5 (PND5) and PND14, using only 3 h of imaging acquisition time. An optimized 3D DTI pulse sequence and appropriate animal setup to minimize physiological motion artifacts are the keys to successful high resolution 3D DTI imaging. Thus, a 3D rapid acquisition relaxation enhancement DTI sequence with twin navigator echoes was implemented to accelerate imaging acquisition time and minimize motion artifacts. It has been suggested that neonatal mammals possess a unique ability to tolerate mild-to-moderate hypothermia and hypoxia without long term impact. Thus, we additionally utilized this ability to minimize motion artifacts in magnetic resonance images by carefully suppressing the respiratory rate to around 15/min for PND5 and 30/min for PND14 using mild-to-moderate hypothermia. These imaging strategies have been successfully implemented to study how the effect of cocaine exposure in dams might affect brain development in their rat pups. Image quality resulting from this *in vivo* DTI study was comparable to *ex vivo* scans. fractional anisotropy values were also similar between the live and fixed brain scans. The capability of acquiring high quality *in vivo* DTI imaging offers a valuable opportunity to study many neurological disorders in brain development in an authentic living environment.

Keywords: magnetic resonance imaging, diffusion tensor imaging, brain development, white matter, neonatal rats

INTRODUCTION

High resolution non-invasive imaging on live neonatal rodents is a highly desirable tool in neurological development studies, as it can provide full representation of 3D neuroanatomy and allow for longitudinal studies. The spatio-temporal maturation pattern of the rodent brain obtained using such neuroimaging methods affords valuable information in the identification of normal, as well as abnormal, brain developmental features. Magnetic resonance (MR) diffusion tensor imaging (DTI) is a quantitative and non-invasive imaging technique reflecting the magnitude and direction of water molecule diffusion in tissues. DTI offers a unique non-invasive window into the process of brain maturation (Le Bihan et al., 1986; Basser and Pierpaoli, 1996) using a set of water diffusion related parameters, including fractional anisotropy (FA), radial diffusivity (RD), axial diffusivity (AD), and mean diffusivity (MD). FA reflects water diffusion anisotropy due to the differences among diffusitivities along the three principal directions. As a result of the presence of orderly arranged axon and myelin sheaths within white matter fiber tracts, FA values are usually higher in white matter structures than surrounding brain regions. MD is an averaged measure of local water diffusivity.

Due to the presence of myelin sheaths and microstructural components of axons in white matter, water molecules move more freely along than perpendicularly to the long axis of the white matter fiber. This phenomenon is known as anisotropic diffusion. Though anisotropic diffusion can still be detected in a white matter dysmyelination mouse model (shiverer mice), it is significantly lower in the fixed brains of shiverer mice than that of wild-type (Tyszka et al., 2006). It has been suggested that both myelination and intact axon structures contribute to diffusion anisotropy (Mori et al., 2001; Neil et al., 2002; Zhang et al., 2003; Tyszka et al., 2006). Thus, data gleaned from DTI is directly linked to the anatomic organization and microstructural features of white matter fiber tracts (Basser et al., 1994); information that cannot be obtained through conventional MRI T1 or T2 images.

Aside from traditional DTI techniques, 3D high resolution DTI MRI (Adolph, 1948) on intact rodent brains provides a 3D characterization of tissue samples in a non-destructive way and therefore is free from sectioning-related artifacts (Mori et al., 2001)

when compared to histological methods. Moreover, unlike the labor intensive histological methods, high resolution 3D DTI of the whole brain is obtained during one scan session and can be "sliced" in any orientation desired. Therefore, it potentially plays an important role in neonatal developmental studies (Neil et al., 1998; Mori et al., 2001; Zhang et al., 2003; Bockhorst et al., 2008). Since DTI MR imaging utilizes strong magnetic gradients to generate imaging contrast based on small water molecule diffusion, it is inherently extremely sensitive to motion induced artifacts. Furthermore, in order to acquire high resolution DTI images, historically, long acquisition times (>10 h) have to be utilized for both diffusion and spatial encoding. These two major limitations make 3D DTI imaging difficult for live animals (Schick, 1997; Mori and van Zijl, 1998; Xue et al., 1999; Mori et al., 2001).

Thus far, most studies have been performed in *ex vivo* fixed brain specimen (Zhang et al., 2003, 2005; Verma et al., 2005; Tyszka et al., 2006; Huang et al., 2008; Aggarwal et al., 2010; Jiang and Johnson, 2010). DTI imaging on live neonatal rodents offers many advantages over fixed brain specimen scans. First, it provides information in an authentic physiological environment without the effects of brain fixation. Second, it allows for a longitudinal follow-up study to probe the temporal change of brain development or disease progress in the same animals, leading to more statistical power without the need of sacrificing a large number of animals.

Currently, efforts have been made toward DTI imaging of live rodents. However, most of these studies are multi-slice 2D DTI imaging-based, using either conventional spin echo or echo planar imaging (EPI) spin echo sequences (Sun et al., 2003, 2005; Chahboune et al., 2007, 2009; Bockhorst et al., 2008; Kim et al., 2009). Compared with 3D acquisition mode, it is difficult to achieve less than 0.5 mm through-plane resolution in such images, due to the limitation of the radio-frequency (RF) excitation slice profile in 2D acquisition. For perspective, it has been demonstrated that 0.5 mm is in the range of the width of corpus callosum (from 0.327 to 0.751 mm) of 3-month Purdue-Wistar rats (Fitch et al., 1990). Many studies have shown that spatial resolution can affect the accuracy of FA calculation (Kim et al., 2006). Additionally, partial-volume-effects can lead to an underestimation of FA, and thus inaccurate assessment of spatio-temporal changes of white matter. This problem, which is exacerbated particularly in the neonatal rodent brain due to its small size, can be mitigated by high resolution 3D imaging. Thus far, only a few studies have successfully performed 3D DTI imaging in live adult rodent brains using a DTI rapid acquisition relaxation enhancement (RARE) based approach (Xue et al., 1999; Aggarwal et al., 2010). Due to the high respiratory rates of neonatals, it is even more challenging to achieve high resolution DTI in neonatal rat pups.

In this study, we have investigated tactics which may facilitate the acquisition of high resolution 3D DTI imaging in neonatal rats. We have found that an optimized 3D DTI RARE method, with motion and eddy current artifacts correction using twin navigator echoes phase correction strategy (Xue et al., 1999), can allow for a 3D DTI acquisition within a few hours (~3 h). It has been suggested that mammalian neonatal can tolerate mild-to-moderate hypothermia and hypoxia when compared to their adult counterparts (Adolph, 1969; Singer, 1999). Thus, we used mild-to-moderate hypothermia to minimize motion artifacts in MR images by carefully suppressing the respiratory rate to 15/min for postnatal day 5 (PND5) and 30/min for PND14. In this paper, we explored the feasibility of acquiring high resolution 3D DTI images in live neonatal rats at two different ages using these strategies. Image quality and various DTI parameters of the live neonatal rat scans were compared with those of postmortem fixed brain scans at the same ages.

MATERIALS AND METHODS

MRI PULSE SEQUENCE

Conventional 3D Stejskal–Tanner spin echo DTI acquisition can achieve high resolution images. However, the long acquisition time (10 h or more) and highly motion-sensitive nature limit its usage mainly on postmortem imaging. Two major DTI acquisition approaches, diffusion weighed EPI/SPIRAL (DW–EPI/SPIRAL) and diffusion weighed rapid acquisition relaxation enhancement (DW–RARE) methods, can be employed to accelerate the acquisition time by a factor of 2–10 when compared to the conventional diffusion weighed spin echo pulse sequence (Turner and Lebihan, 1990; Muller et al., 1994; Schick, 1997; Mori and van Zijl, 1998; Pipe et al., 2002; Liu et al., 2004; Frank et al., 2010). By refocusing the echoes using a series of 180° RF pulses, the advantage of DW–RARE over the DW–EPI/SPIRAL pulse sequence is that it is less sensitive to signal loss and image distortion caused by the field inhomogeneity, a feature that is critically important for small-animal high resolution 3D DTI study using high magnetic fields (Pipe et al., 2002; Deng et al., 2008; Sarlls and Pierpaoli, 2008). However, motion artifacts augmented by the diffusion sensitizing gradients may degrade image quality through the different magnetization pathways generated by multiple 180° RF pulses for the DW–RARE method. Proper strategies need to be taken to minimize such artifacts.

Similar to the approach proposed by Mori and van Zijl (1998), a 3D DTI RARE sequence with twin navigator echoes was implemented on a Bruker horizontal bore 9.4 T scanner (BioSpec 9.4/30 USR, Bruker Biospin, Billerica, MA, USA). A pair of diffusion gradients was applied around the first 180° RF pulse. The strength and direction of diffusion gradients were set according to the input b value and diffusion directions. Moreover, to remove the stimulated echo pathways that did not have correct diffusion encoding, crusher gradients with varying magnitudes and polarities were applied around each 180° refocusing RF pulse. The bandwidth of the 180° refocus RF pulse was set at two to three times larger than that of the excitation 90° RF pulse to minimize the stimulated echoes induced by the imperfect refocus pulse. Two navigator echoes were acquired after the imaging echoes to correct for motion and eddy current artifacts (Mori and van Zijl, 1998). The acquisition parameters were: TR = 700 ms; the first RARE echo was assigned to the k-space center, effective TE = 23.662 ms; RARE echo spacing = 11.9 ms.

The total imaging time is inversely proportionate to the RARE factor. However, we cannot use a very high RARE factor in this DTI RARE sequence due to the fact that the stimulated echo pathway in high RARE factor readout becomes more complex and difficult to be removed, leading to the poor image quality. Using phantom studies, we empirically determined that a RARE factor of three

yields a good trade-off between acquisition speed and sharpness of images for *in vivo* neonatal animal scans.

Diffusion gradient duration $\delta = 6.5$ ms, diffusion gradient separation $\Delta = 12.72$ ms, field of view (FOV) = 27 mm × 19.2 mm × 11 mm, matrix size = 180 × 128 × 55, the resolution = 0.15 mm × 0.15 mm × 0.2 mm, readout direction: H–F, phase encoding direction: L–R, slab encoding direction: A–P. The twin navigator echoes were used to correct for the phase incoherence between the odd and even echoes to alleviate the motion and eddy current effects (Mori and van Zijl, 1998). A 72-mm volume coil and a surface coil were used for RF transmission and signal receiving, respectively, under an actively decoupled cross-coil routine mode. Finally, the data was interpolated to the final matrix size 360 × 256 × 128 to achieve a nominal spatial resolution around 0.075 mm × 0.075 mm × 0.1 mm.

IN VIVO ANIMAL SCAN

This methods described were designed for a study (P01DA022446) to determine how the effect of prenatal cocaine exposure may affect a rat pup's brain development. The animal scanning protocol was approved by Institutional Animal Care and Use Committee (IACUC) of University of North Carolina at Chapel Hill. Twelve Sprague-Dawley PND5 (average weight 9.6 ± 1.1 g) and 30 PND14 (average weight 32.3 ± 2.3 g) rats were studied. Male and female subjects were in pairs from the same litter. Anesthesia was induced using 3% isoflurane mixed with oxygen. For maintaining anesthesia in neonatal rats, isoflurane level was adjusted in the range of 0.6–1.5 to keep the respiratory rate within a target range. The body surface of PND5 pups was covered in 100% pure petroleum jelly (Vi-Jon Laboratories, Inc, St. Louis, MO 63114, USA) to prevent skin dehydration during image acquisition. The lower jaw of PND5 pups was secured to reduce the bulk of the motion, and reinforced by padding around the head. The room temperature of the MR scanner room was set at 22°C. Animal respiration and surface body temperature were continuously monitored using a MR compatible small-animal monitoring system SAII 1025L (SAII Instruments, Inc, Stony Brook, NY 11790, USA). In this study, body surface temperatures were obtained from abdomen region, and maintained in the range of 24–26°C and 33°C for PND5 and PND14 pups, respectively, using a circulating water heating system. Thus, since the normal body surface temperature of rat pups ranges from 35 to 37°C, the PND5 and PND14 pups were under moderate and mild hypothermic conditions, respectively. Respiratory rates were maintained at about 15/min and 30/min in PND5 and PND14 pups, respectively. A mouse head surface coil and a rat head phase array surface coil were used for imaging PND5 and PND14 rat pups, respectively. Six non-collinear diffusion encoding directions with $b = 1000$ s/mm^2 images and one baseline reference $b = 0$ image were acquired for the *in vivo* DTI scans. The diffusion b values were set to 1000 s/mm^2 for the *in vivo* scans. The total scan time was 3 h 10 min, which is reduced by a factor of three compared to conventional DW–SE pulse sequences used to acquire the same resolution DTI images.

POSTMORTEM FIXED BRAIN SCAN

Tissues were collected from both PND5 and PND14 rats following standard cardiac puncture perfusions while under anesthesia [150 g/kg sodium pentobarbital (sigma)], first with 1.5 mL/min phosphate-buffered saline (PBS) followed by 1.5 mL/min 4% paraformaldehyde. The intact head was then excised and placed in 4% paraformaldehyde. The specimens were placed in PBS solution and stored at 4°C at least 12 h before MR imaging. All fixed tissue was equilibrated to room temperature for several hours prior to imaging of the whole head. The sample temperatures were measured to be 21 ± 0.2°C. Similar acquisition parameters of 3D DTI RARE pulse sequence were used for DTI acquisition in fixed brain specimen. In total, one baseline reference scan and 21 diffusion encoding directions were utilized. Since the paraformaldehyde fixation reduces water mobility in tissue (Sun et al., 2003, 2005), a higher b value ($b = 1600$ s/mm^2) was utilized for the postmortem fixed brain DTI. The fixed brains were scanned at room temperature and the total image acquisition time was about 10 h.

COMPARISON BETWEEN *IN VIVO* AND *EX VIVO* SCANS

Since the postmortem scans were free of physiological motion-related artifacts, these scans were used to quantitatively evaluate the image quality of the *in vivo* scans. Two independent raters performed their evaluation by examining the extent of motion artifact, signal loss in images, overall noise, and other artifacts in multiple brain regions. Using the fixed brain specimen DTI scans as references, *in vivo* DTI images with very little motion artifact, negligible ringing artifact, and little or no signal loss were rated good, or otherwise rated poor. Scan successful rate was defined as the ratio of good data set to total data set.

The signal to noise ratio (SNR) in the $b = 0$ reference and diffusion scans was computed and compared between images acquired from the *in vivo* and *ex vivo* scans. The chemical fixation procedure changed many tissue MR properties, including T1, T2, and ADC, leading to altered MR signal intensity in the images of the fixed postmortem brains (Sun et al., 2003, 2005; Yong-Hing et al., 2005; Shepherd et al., 2009). Taking these factors into consideration in the SNR comparison, we computed the adjusted SNR for the *ex vivo* fixed brain as $\mathrm{SNR}_{\mathrm{adjusted}} = S_{\mathrm{adjusted}}/\sigma$, where σ is the SD of the background Gaussian noise, and S_{adjusted} is the adjusted MR signal. The adjust MR signal is computed as

$$S_{\mathrm{adjusted}} = S\left(\frac{M0_{\mathrm{live}}}{M0_{\mathrm{fixed}}}\right) \mathrm{e}^{b\cdot D_{\mathrm{fixed}}}\, \mathrm{e}^{-b\cdot D_{\mathrm{live}}}\, \mathrm{e}^{\frac{\mathrm{TE}}{T2_{\mathrm{fixed}}}}\, \mathrm{e}^{-\frac{\mathrm{TE}}{T2_{\mathrm{live}}}} \times \frac{1-\mathrm{e}^{-\frac{\mathrm{TR}}{T1_{\mathrm{live}}}}}{1-\mathrm{e}^{-\frac{\mathrm{TR}}{T1_{\mathrm{fixed}}}}},$$

where S is the measured MR signal from the postmortem brain, and the subscripts "fixed" and "live" refer to the MR properties for the fixed and live tissues, respectively.

Assuming a D_{live} of 1×10^{-3} mm^2/s, a $T1_{\mathrm{live}}$ of 1800 ms, a $T2_{\mathrm{live}}$ of 40 ms and a proton density $M0_{\mathrm{live}}$ of 1.0 for the *in vivo* scans, and a D_{fixed} of 0.3×10^{-3} mm^2/s, a $T1_{\mathrm{fixed}}$ of 1400 ms, a $T2_{\mathrm{fixed}}$ of 32 ms and a proton density $M0_{\mathrm{fixed}}$ of 0.85 for the *ex vivo* scans using previously published literature values (de Graaf et al., 2006; Shepherd et al., 2009), we computed $\mathrm{SNR}_{\mathrm{adjusted}}$ for the *ex vivo* images. A two tail t-test was used to compare FA, MD, and SNR between the *in vivo* and *ex vivo* scans.

All DTI data were processed using DTI Studio software (www.mristudio.org). MD and FA were computed using ROIs

ranging from 20 to 24 pixels (0.0113–0.0135 mm^3), placed in the genu of corpus callosum (gcc), body of corpus callosum (bcc), splenium of corpus callosum (scc). DTI tractography was performed using the gcc ROI as the seed point, and the tracking algorithm was terminated when the FA value was below 0.25. The allowed maximum turn angle for adjacent voxels was set to 70° to minimize the occurrence of spurious fiber orientations caused by noise.

RESULTS

All PND5 and PND14 rat pups recovered 10–30 min after MR scans (∼3.5 h) with a zero mortality rate. Representative *in vivo* images and *ex vivo* brain DTI images are demonstrated in **Figure 1** and the computed diffusion indices, such as FA and MD are shown in **Figure 2**. The two independent raters had the same ratings in 40 out of a total of 42 scans (a 95.2% agreement). For the two cases that two raters initially disagreed, consensus was reached after discussion. After reaching consensus, images acquired from 10 out of 12 PND5 and 27 out of 30 PND14 rats were rated as "good," resulting in success rates of 83 and 90% for the PND5 and PND14 pups, respectively. Though the overall image quality of the *in vivo* scans was comparable to that of the *ex vivo* scans, more ringing artifacts were observed in the $b = 0$ and diffusion weighted raw images as demonstrated in **Figure 1**. However, these remaining artifacts have very little effect on DTI indices as shown in **Figure 2**.

As shown in **Figure 2**, major white matter fibers depicted in the FA maps were similar between the *in vivo* and the *ex vivo* scans. Conversely, the contrast between gray and white matter was more pronounced in the *ex vivo* than in the *in vivo* MD images, suggesting that MD had a greater reduction within white matter during the chemical fixation.

Figure 3 demonstrates the efficacy of motion correction using the twin navigator echoes. Due primarily to respiration and pulsatile motion of large blood vessels near the ventral side, it was expected that more motion artifact might occur in slices close to the ventral side (**Figure 3C**) when compared to the dorsal side of the head (**Figure 3A**). After the twin navigator echo motion correction, signal loss was recovered, and the background noise was reduced as marked by the arrows in **Figures 3B,D**. Though DTI image quality has been improved after the dual echo navigator correction, some residual motion artifacts can still be observed.

Tables 1 and **2** shows the FA and MD values from the *in vivo* and *ex vivo* scans in several anatomical regions: gcc, bcc, scc. There was no statistically significant difference in the FA value between the *in vivo* and the *ex vivo* scans, while MD values were significantly lower ($P < 0.05$) in the *ex vivo* scans, in agreement with previous findings (Sun et al., 2003, 2005). Moreover, there was no

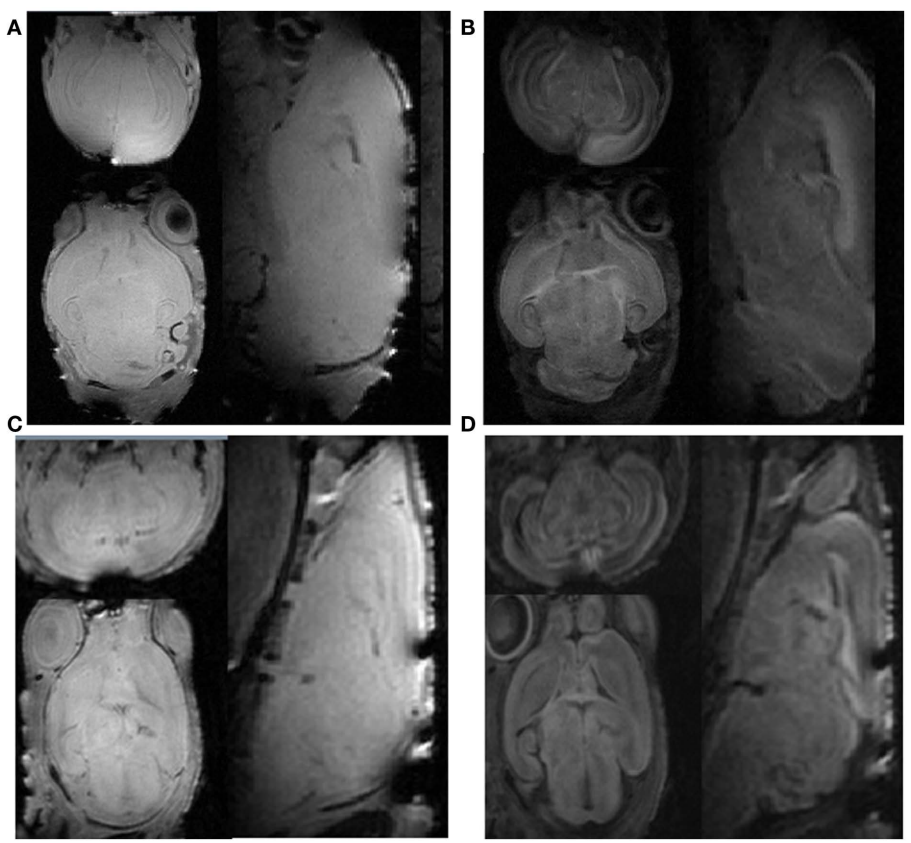

FIGURE 1 | The comparison of $b = 0$ and diffusion weighted images between the *ex vivo* scan and the *in vivo* scans. (A) *Ex vivo* baseline $b = 0$ image; **(B)** *ex vivo* diffusion weighted image; **(C)** *in vivo* baseline $b = 0$ image; **(D)** *in vivo* diffusion weighted image. The axial, sagittal, and coronal plane images are shown clockwise.

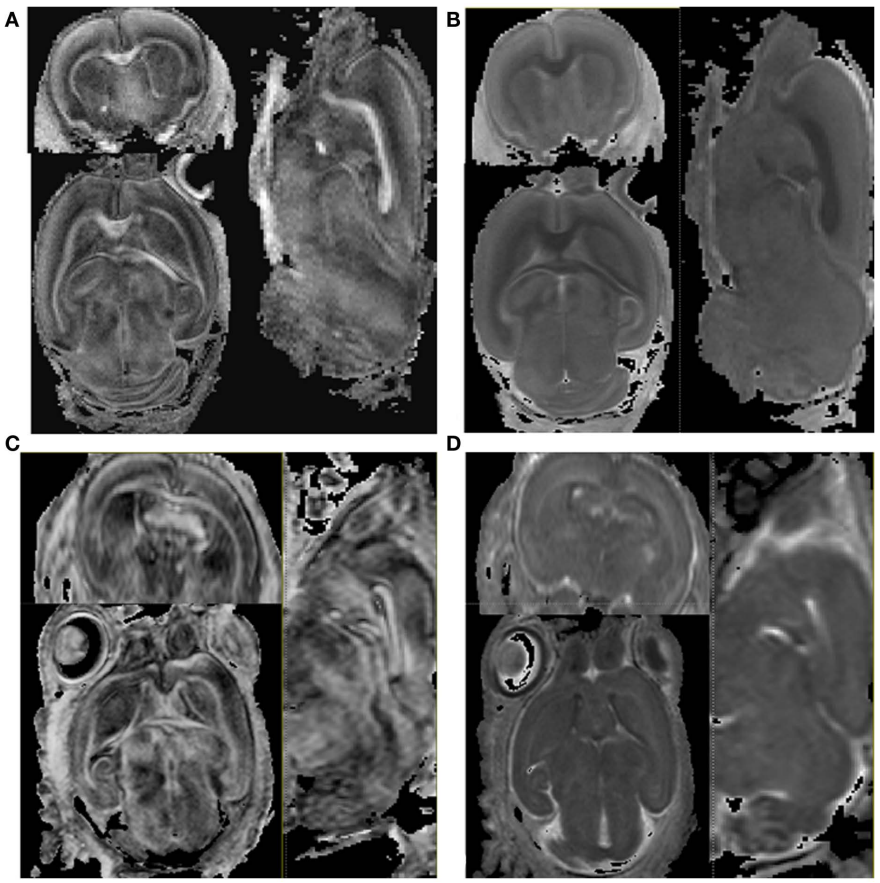

FIGURE 2 | The comparison of FA and MD maps between the *ex vivo* and the *in vivo* scan. (A) *Ex vivo* baseline image. **(B)** *Ex vivo* diffusion weighted image **(C)** *in vivo* baseline image **(D)** *in vivo* diffusion weighted image. The axial, sagittal, and coronal plane images are shown clockwise.

significant difference between the SNR of the *in vivo* scans and the adjusted SNR of the *ex vivo* scans for both the baseline and diffusion weighted images, as shown in **Table 3**.

Figure 4 shows the fiber tracking results in live and postmortem fixed brain DTI images. The major fiber bundle of corpus callosum can be readily obtained in PND5 and PND14 live DTI images. The tracked fibers showed very similar patterns between the *in vivo* and the *ex vivo* scans for both the PND5 and PND14 groups.

DISCUSSION

Recent studies have shown that a Periodically Rotated Overlapping ParallEL Lines with Enhanced Reconstruction (PROPELLER) and its recent modified form with split acquisition of fast spin echo signal for diffusion imaging (SPLICE) pulse sequence techniques (Schick, 1997; Deng et al., 2008) are intrinsically motion insensitive because these methods are self-navigated. These techniques have been successfully applied for abdominal DTI study. Though this is a very promising technique, it has several limitations. First, 1.5 times longer image acquisition time is needed for PROPELLER acquisition compared with conventional sampling for a 2D acquisition (Pipe et al., 2002). To achieve a high resolution 3D DTI, blade sampling needs to be performed on a 3D sphere, resulting in a dramatically increased image acquisition time. Second, non-Cartesian k-space sampling is utilized in PROPELLER and SPLICE methods. The k-space regridding is usually required for image reconstruction and any system imperfection will cause image blurring by degrading the point spread function of k-space. In contrast, the DTI RARE sequence uses multiple 180° pulses to refocus the signal and a Cartesian k-space sampling is obtained. This approach is not sensitive to geometric distortion and signal reduction caused by background susceptibility artifacts. The image reconstruction is straightforward and rapid. The disadvantage of DTI RARE is its sensitivity to motion artifacts. By physically suppressing the respiratory motion using hypothermia together with twin navigator echo motion correction, we have demonstrated that high quality DTI images can be obtained *in vivo* from rat pups. In our study, the experimentally measured SNR of *in vivo* scans is only slightly lower than that of the *ex vivo* scans, further indicating that the image quality of the *in vivo* rat pup scans are comparable to that of the postmortem fixed *ex vivo* brain scans.

DIFFUSION ENCODING DIRECTIONS

In this study, we used 21 and 6 non-collinear diffusion gradient directions for the *ex vivo* and *in vivo* scans, respectively. More diffusion encoding directions could be used for the *in vivo* study if a longer DTI image acquisition time was possible. Six diffusion

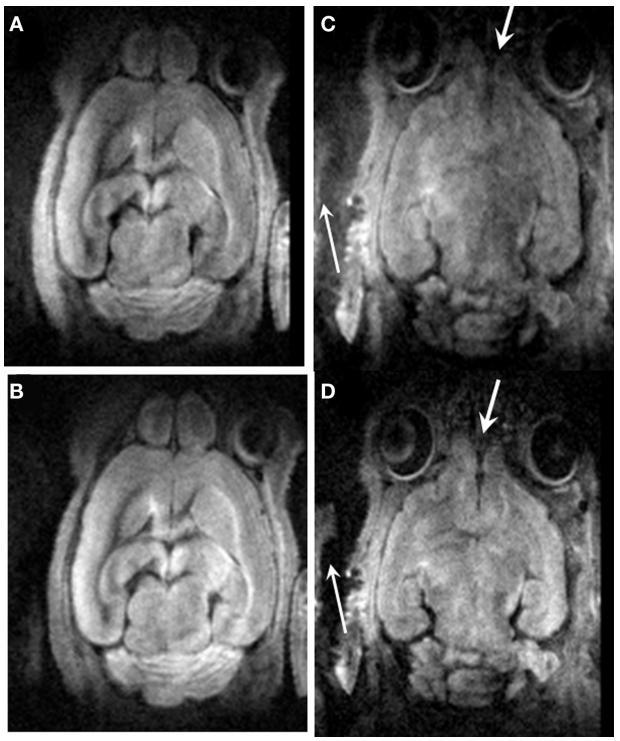

FIGURE 3 | The comparison before and after twin navigator echo correction. (A) A slice of the dorsal side before **(A)** and after **(B)** correction; **(C)** a slice of the ventral side before **(C)** and after **(D)** correction. Motion artifacts were minimized after the twin navigator echo correction as marked by the arrow.

Table 1 | Fractional anisotropy comparison between the *in vivo* and the *ex vivo* scans for PND5 and PND14 rat pups.

	PND5 (*in vivo*)	PND5 (*ex vivo*)	PND14 (*in vivo*)	PND14 (*ex vivo*)
GCC	0.73 ± 0.034	0.74 ± 0.022	0.78 ± 0.053	0.80 ± 0.029
BCC	0.55 ± 0.039	0.56 ± 0.028	0.56 ± 0.086	0.58 ± 0.042
SCC	0.79 ± 0.037	0.80 ± 0.019	0.81 ± 0.045	0.81 ± 0.021

Fractional anisotropy values were not significantly different between the in vivo and ex vivo scans.

Table 2 | Mean diffusivity (unit: 10^{-3} mm^2/s) comparison between *in vivo* and *ex vivo* scans for PND5 and PND14 scans.

	PND5 (*in vivo*)	PND5 (*ex vivo*)	PND14 (*in vivo*)	PND14 (*ex vivo*)
GCC	0.970 ± 0.053*	0.284 ± 0.022	0.734 ± 0.047*	0.233 ± 0.018
BCC	1.120 ± 0.089*	0.394 ± 0.047	0.884 ± 0.086*	0.344 ± 0.031
SCC	0.930 ± 0.055*	0.293 ± 0.026	0.865 ± 0.045*	0.277 ± 0.028

Significant differences were found in MD between the in vivo and the ex vivo scans ($P < 0.05$).*

Table 3 | Signal to noise ratio comparison between the *in vivo* and the *ex vivo* DTI scan.

	SNR for *in vivo*	$SNR_{adjusted}$ for *ex vivo* scans
$b = 0$ reference images	24.3 ± 3.4	29.4 ± 2.39
Diffusion weighted images	8.3 ± 3.4	10.447 ± 0.865

No significant difference was observed between the in vivo SNR and the adjusted SNR of the postmortem fixed ex vivo scans in both baseline and diffusion images.

encoding directions is the least number of directions for DTI computation assuming a simple ellipsoid tensor model. It does not provide sufficient information to resolve fiber crossing in DTI. The high angular resolution diffusion imaging (HARDI) approach has been proposed to overcome this problem by using a large number of diffusion encoding directions at an expense of increasing the imaging acquisition time (Tuch et al., 2002). We only performed a six diffusion encoding acquisition for *in vivo* scans due to the following reasons. First, we needed to obtain high resolution 3D DTI images with a time constraint of a few hours to reduce the risk of damaging the very young rat pups. Second, based on the established white matter atlas in both human and rodents (Chuang et al., 2011; Nowinski et al., 2011), the white matter tracks in rodent brain do not have as many fiber crossing regions as those in human brain. Third, our study mainly focused on major white matter regions in which fiber crossing is less likely to be found. We qualitatively compared the tracked fiber within major white matter regions such as corpus callosum between the *in vivo* and the *ex vivo* scans. We have found that major white matter fibers in both PND5 and PND14 pups can be readily obtained from the *in vivo* scans using less than one-third of the data acquisition time/diffusion encoding directions when compared to the *ex vivo* fixed brain scans. This suggests that the imaging acquisition tactics developed in this study can be utilized to acquire DTI images in live rat pups reliably and consistently.

MOTION CORRECTION

We adopted the twin navigator echo navigator method developed by Mori and van Zijl (1998) to alleviate the motion effect in our 3D DTI RARE sequence. This approach assumes a constant phase variation between the odd and even echoes induced by motion or eddy current. As demonstrated in **Figure 3**, image quality has been improved with recovered signal and reduced noise after the correction. However, since the assumption of constant phase variation between odd and even echoes did not always hold true in the *in vivo* scans, residual motion artifacts were still observed, as shown in **Figure 3**. To further minimize the motion artifacts, 2D navigator correction (Porter and Heidemann, 2009) may be explored in the future.

We did not use respiratory gating to minimize motion effects for several reasons. The TR of the 3D DTI RARE sequence was kept relatively short (700 ms) to achieve a 3-h total acquisition time and respiratory gating may lengthen image acquisition quite substantially. The respiratory rate of a neonatal rat pup may change during the 3-h acquisition window, leading to variations in the effective TR. If TR is short (as in our study), these variations are not negligible, and can result in signal variations and inaccurate calculation of DTI indices. In our study, we found that respiration

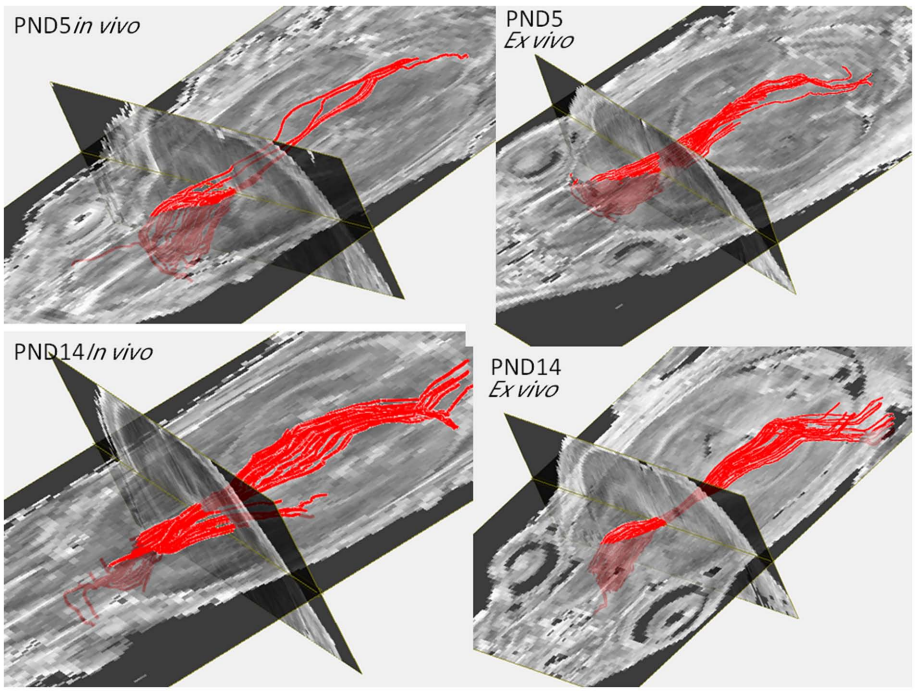

FIGURE 4 | Fiber tractography obtained from the *in vivo* and the *ex vivo* PND5 and PND14 pups.

gating did not yield good quality images if the respiratory rate is high. On the other hand, suppressing respiratory rates without gating was adequate to achieve virtually motion artifacts free images.

It is more challenging to acquire high quality 3D DTI images in live PND5 pups compared to PND14 rats. It has been suggested that mammalian neonatal can tolerate severe hypoxia and hypothermia for a longer time compared to their adult counterparts (Adolph, 1969; Singer, 1999). In a study investigating the survival rate of neonatal rats in a pure nitrogen environment (Adolph, 1969), Adolph demonstrated that 0 to 5-day-old rats could survive in such an environment for 1–2 h when the colonic temperature was cooled down to 8–10°C, while in 11 to 16-day-old rats, the optimal body temperature for survival increased to 20°C and endurance time decreased to 0.5 h. These findings provided the base of utilizing hypothermia for PND5 DTI. The neuroprotective effects of the mild-to-moderate hypothermia have been firmly established (Adolph, 1969; Blackmon and Stark, 2006). Additionally, hypothermia reduces the metabolic rate and further minimizes physiological motion. In our study, we found that a low level of isoflurane (0.6–0.8%) in conjunction with hypothermia was sufficient to keep most PND5 pups under anesthesia and to maintain a respiratory rate around 15/min.

OTHER ISSUES

The direct advantage of improving the resolution is to reduce the partial volume effect, making the diffusion indices calculation more accurate. Lee et al. (2006) reported much lower FA values in major white matter using low resolution DTI images (∼1 mm in plane and 0.5 through-plane resolution) at 1.5 T. They correctly ascribe it to the partial volume effect. The mean FA values of corpus callosum in our study are higher than those in a brain development study to investigate the temporal change of DTI indices from PND0 to PND56 rats reported by Bockhorst et al. (2008) using a spatial resolution of 0.27 mm × 0.27 mm × 0.5 mm.

A higher RARE factor could further increase the speed of image acquisition. However, the stimulated echo pathway becomes more complex and more difficult to be removed along with an increase of RARE factor, leading to the poor image quality. In an empirical phantom study, we found that a RARE factor of three was a good trade-off between acquisition speed and sharpness of images for *in vivo* neonatal animal scans (data not shown). To further improve the speed of the image acquisition, a 3D diffusion weighed gradient and spin echo (3D DW–GRASE) could be implemented. The GRASE sequence is a combination of segmented EPI and fast spin echo, interleaving the short EPI echo readout train with RF refocusing pulses. A 3D DW–GRASE provides a compromise between signal loss due to the field inhomogeneity in gradient echoes and the interference of stimulated echoes by refocus RF pulses in spin echoes. Aggarwal et al. (2010) have explored a DW–GRASE approach that yields a four times acceleration using two refocus pulses and two gradient echoes.

CONCLUSION

In this study, we have demonstrated that an optimized 3D DTI RARE approach and an appropriate animal setup minimizing respiration motion are the keys to achieving high quality 3D DTI images in live animals. Taking advantage of the distinct physiological characteristic that neonatal rats can survive low body temperatures, we have demonstrated that mild-to-moderate

hypothermia can be utilized to suppress physiological motion artifacts to achieve good quality DTI images.

ACKNOWLEDGMENTS

The work described was supported in part by awards P01DA022446 (Josephine M. Johns) and F31DA026251 (Martin A. Styner) from the National Institutes on Drug Abuse. The content is solely the responsibility of the authors and does not necessarily represent the official views of the National Institutes on Drug Abuse or the National Institutes of Health. We thank Drs. Susumu Mori and Jiangyang Zhang for their valuable suggestions regarding the MR pulse sequence. NICHD P30 HD03110 awarded to J. Piven.

REFERENCES

Adolph, E. (1948). Tolerance to cold and anoxia in infant rats. *Am. J. Physiol.* 155, 366–377.

Adolph, E. F. (1969). Regulations during survival without oxygen in infant mammals. *Respir. Physiol.* 7, 356–368.

Aggarwal, M., Mori, S., Shimogori, T., Blackshaw, S., and Zhang, J. Y. (2010). Three-dimensional diffusion tensor microimaging for anatomical characterization of the mouse brain. *Magn. Reson. Med.* 64, 249–261.

Basser, P. J., Mattiello, J., and LeBihan, D. (1994). MR diffusion tensor spectroscopy and imaging. *Biophys. J.* 66, 259–267.

Basser, P. J., and Pierpaoli, C. (1996). Microstructural and physiological features of tissues elucidated by quantitative-diffusion-tensor MRI. *J. Magn. Reson. B.* 111, 209–219.

Blackmon, L. R., and Stark, A. R. (2006). Hypothermia: a neuroprotective therapy for neonatal hypoxic-ischemic encephalopathy. *Pediatrics* 117, 942–948.

Bockhorst, K. H., Narayana, P. A., Liu, R., Vijjula, P. A., Ramu, J., Kamel, M., Wosik, J., Bockhorst, T., Hahn, K., Hasan, K. M., and Perez-Polo, J. R. (2008). Early postnatal development of rat brain: in vivo diffusion tensor imaging. *J. Neurosci. Res.* 86, 1520–1528.

Chahboune, H., Ment, L. R., Stewart, W. B., Ma, X. X., Rothman, D. L., and Hyder, F. (2007). Neurodevelopment of c57b/l6 mouse brain assessed by in vivo diffusion tensor imaging. *NMR Biomed.* 20, 375–382.

Chahboune, H., Ment, L. R., Stewart, W. B., Rothman, D. L., Vaccarino, F. M., Hyder, F., and Schwartz, M. L. (2009). Hypoxic injury during neonatal development in murine brain: correlation between in vivo DTI findings and behavioral assessment. *Cereb. Cortex* 19, 2891–2901.

Chuang, N., Mori, S., Yamamoto, A., Jiang, H., Ye, X., Xu, X., Richards, L. J., Nathans, J., Miller, M. I., Toga, A. W., Sidman, R. L., and Zhang, J. (2011). An MRI-based atlas and database of the developing mouse brain. *Neuroimage* 54, 80–89.

de Graaf, R. A., Brown, P. B., McIntyre, S., Nixon, T. W., Behar, K. L., and Rothman, D. L. (2006). High magnetic field water and metabolite proton t1 and t2 relaxation in rat brain in vivo. *Magn. Reson. Med.* 56, 386–394.

Deng, J., Omary, R. A., and Larson, A. C. (2008). Multishot diffusion-weighted splice propeller MRI of the abdomen. *Magn. Reson. Med.* 59, 947–953.

Fitch, R. H., Berrebi, A. S., Cowell, P. E., Schrott, L. M., and Denenberg, V. H. (1990). Corpus callosum: effects of neonatal hormones on sexual dimorphism in the rat. *Brain Res.* 515, 111–116.

Frank, L. R., Jung, Y., Inati, S., Tyszka, J. M., and Wong, E. C. (2010). High efficiency, low distortion 3d diffusion tensor imaging with variable density spiral fast spin echoes (3d dw vds rare). *Neuroimage* 49, 1510–1523.

Huang, H., Yamamoto, A., Hossain, M. A., Younes, L., and Mori, S. (2008). Quantitative cortical mapping of fractional anisotropy in developing rat brains. *J. Neurosci.* 28, 1427–1433.

Jiang, Y., and Johnson, G. A. (2010). Microscopic diffusion tensor imaging of the mouse brain. *Neuroimage* 50, 465–471.

Kim, J. H., Haldar, J., Liang, Z. P., and Song, S. K. (2009). Diffusion tensor imaging of mouse brain stem and cervical spinal cord. *J. Neurosci. Methods* 176, 186–191.

Kim, M., Ronen, I., Ugurbil, K., and Kim, D. S. (2006). Spatial resolution dependence of dti tractography in human occipito-callosal region. *Neuroimage* 32, 1243–1249.

Le Bihan, D., Breton, E., Lallemand, D., Grenier, P., Cabanis, E., and Laval-Jeantet, M. (1986). MR imaging of intravoxel incoherent motions: application to diffusion and perfusion in neurologic disorders. *Radiology* 161, 401–407.

Lee, F. K., Fang, M. R., Antonio, G. E., Yeung, D. K., Chan, E. T., Zhang, L. H., Yew, D. T., and Ahuja, A. T. (2006). Diffusion tensor imaging (DTI) of rodent brains in vivo using a 1.5t clinical MR scanner. *J. Magn. Reson. Imaging* 23, 747–751.

Liu, C. L., Bammer, R., Kim, D. H., and Moseley, M. E. (2004). Self-navigated interleaved spiral (snails): application to high-resolution diffusion tensor imaging. *Magn. Reson. Med.* 52, 1388–1396.

Mori, S., Itoh, R., Zhang, J. Y., Kaufmann, W. E., van Zijl, P. C. M., Solaiyappan, M., and Yarowsky, P. (2001). Diffusion tensor imaging of the developing mouse brain. *Magn. Reson. Med.* 46, 18–23.

Mori, S., and van Zijl, P. C. M. (1998). A motion correction scheme by twin-echo navigation for diffusion-weighted magnetic resonance imaging with multiple RF echo acquisition. *Magn. Reson. Med.* 40, 511–516.

Muller, M. F., Prasad, P., Siewert, B., Nissenbaum, M. A., Raptopoulos, V., and Edelman, R. R. (1994). Abdominal diffusion mapping with use of a whole-body echo-planar system. *Radiology* 190, 475–478.

Neil, J., Miller, J., Mukherjee, P., and Huppi, P. S. (2002). Diffusion tensor imaging of normal and injured developing human brain – a technical review. *NMR Biomed.* 15, 543–552.

Neil, J. J., Shiran, S. I., McKinstry, R. C., Schefft, G. L., Snyder, A. Z., Almli, C. R., Akbudak, E., Aronovitz, J. A., Miller, J. P., Lee, B. C. P., and Conturo, T. E. (1998). Normal brain in human newborns: apparent diffusion coefficient and diffusion anisotropy measured by using diffusion tensor MR imaging. *Radiology* 209, 57–66.

Nowinski, W. L., Chua, B. C., Yang, G. L., and Qian, G. Y. (2011). Three-dimensional interactive and stereotactic human brain atlas of white matter tracts. *Neuroinformatics.*

Pipe, J. G., Farthing, V. G., and Forbes, K. P. (2002). Multishot diffusion-weighted FSE using propeller MRI. *Magn. Reson. Med.* 47, 42–52.

Porter, D. A., and Heidemann, R. M. (2009). High resolution diffusion-weighted imaging using readout-segmented echo-planar imaging, parallel imaging and a two-dimensional navigator-based reacquisition. *Magn. Reson. Med.* 62, 468–475.

Sarlls, J. E., and Pierpaoli, C. (2008). Diffusion-weighted radial fast spin-echo for high-resolution diffusion tensor imaging at 3t. *Magn. Reson. Med.* 60, 270–276.

Schick, F. (1997). Splice: sub-second diffusion-sensitive MR imaging using a modified fast spin-echo acquisition made. *Magn. Reson. Med.* 38, 638–644.

Shepherd, T. M., Thelwall, P. E., Stanisz, G. J., and Blackband, S. J. (2009). Aldehyde fixative solutions alter the water relaxation and diffusion properties of nervous tissue. *Magn. Reson. Med.* 62, 26–34.

Singer, D. (1999). Neonatal tolerance to hypoxia: a comparative-physiological approach. *Comp. Biochem. Physiol. A Mol. Integr. Physiol.* 123, 221–234.

Sun, S. W., Neil, J. J., Liang, H. F., He, Y. Y., Schmidt, R. E., Hsu, C. Y., and Song, S. K. (2005). Formalin fixation alters water diffusion coefficient magnitude but not anisotropy in infracted brain. *Magn. Reson. Med.* 53, 1447–1451.

Sun, S. W., Neil, J. J., and Song, S. K. (2003). Relative indices of water diffusion anisotropy are equivalent in live and formalin-fixed mouse brains. *Magn. Reson. Med.* 50, 743–748.

Tuch, D. S., Reese, T. G., Wiegell, M. R., Makris, N., Belliveau, J. W., and Wedeen, V. J. (2002). High angular resolution diffusion imaging reveals intravoxel white matter fiber heterogeneity. *Magn. Reson. Med.* 48, 577–582.

Turner, R., and Lebihan, D. (1990). Single-shot diffusion imaging at 2.0 tesla. *J. Magn. Reson.* 86, 445–452.

Tyszka, J. M., Readhead, C., Bearer, E. L., Pautler, R. G., and Jacobs, R. E. (2006). Statistical diffusion tensor histology reveals regional dysmyelination effects in the shiverer mouse mutant. *Neuroimage* 29, 1058–1065.

Verma, R., Mori, S., Shen, D. G., Yarowsky, P., Zhang, J. Y., and Davatzikos, C. (2005). Spatiotemporal maturation patterns of murine brain quantified by diffusion tensor MRI and deformation-based morphometry. *Proc. Natl. Acad. Sci. U.S.A.* 102, 6978–6983.

Xue, R., van Zijl, P. C. M., Crain, B. J., Solaiyappan, M., and Mori, S.

(1999). In vivo three-dimensional reconstruction of rat brain axonal projections by diffusion tensor imaging. *Magn. Reson. Med.* 42, 1123–1127.

Yong-Hing, C. J., Obenaus, A., Stryker, R., Tong, K., and Sarty, G. E. (2005). Magnetic resonance imaging and mathematical modeling of progressive formalin fixation of the human brain. *Magn. Reson. Med.* 54, 324–332.

Zhang, J. Y., Miller, M. I., Plachez, C., Richards, L. J., Yarowsky, P., van Zijl, P., and Mori, S. (2005). Mapping postnatal mouse brain development with diffusion tensor microimaging. *Neuroimage* 26, 1042–1051.

Zhang, J. Y., Richards, L. J., Yarowsky, P., Huang, H., van Zijl, P. C. M., and Mori, S. (2003). Three-dimensional anatomical characterization of the developing mouse brain by diffusion tensor microimaging. *Neuroimage* 20, 1639–1648.

Conflict of Interest Statement: The authors declare that the research was conducted in the absence of any commercial or financial relationships that could be construed as a potential conflict of interest.

Received: 26 February 2011; accepted: 21 September 2011; published online: 10 October 2011.

Citation: Cai Y, McMurray MS, Oguz I, Yuan H, Styner MA, Lin W, Johns JM and An H (2011) Use of high resolution 3D diffusion tensor imaging to study brain white matter development in live neonatal rats. Front. Psychiatry ***2****:54. doi: 10.3389/fpsyt.2011.00054*

This article was submitted to Frontiers in Child and Neurodevelopmental Psychiatry, a specialty of Frontiers in Psychiatry.